Sustainable Food Technology

ROYAL SOCIETY OF CHEMISTRY

PAPER

View Article Online
View Journal

Cite this: DOI: 10.1039/d5fb00712g

Ho Wood (*Cinnamomum camphora*) essential oil nanoemulsion as a natural alternative combined with UV-C LED for *Staphylococcus aureus* reduction in plant-based burger analogues

Bruno Dutra da Silva,[*ab] Ana Carolina de Morais Mirres,[abc] Ana Julia Bento do Amaral,[abd] Carolina Ramos[abe] and Carlos Adam Conte-Junior[abcde]

The combination of emerging preservation technologies has been the subject of frequent study in recent years. This study evaluated the antimicrobial efficacy of a Ho Wood essential oil nanoemulsion (nHWEO) combined with UV-C LED irradiation for the preservation of plant-based burger analogues. The nanoemulsion prepared with a high-shear homogenizer had an initial droplet diameter of 17.16 ± 6.23 nm. Taken together, the results demonstrate that the small initial droplet diameter favored the system's kinetic stability over 38 days at 4 °C (48.84 nm) and 25 °C (98.74 nm), indicating that the system retained typical nanoemulsion characteristics throughout the evaluation period. The nanoemulsion exhibited greater antimicrobial activity against *Staphylococcus aureus*, with a minimum inhibitory concentration (MIC) of 4.31 mg mL^{-1}, which is lower than that of the free oil (MIC > 4.31 mg mL^{-1}). In the antibacterial activity assay on plant-based burger analogues, treatment with UV-C LED alone (0.32 J cm^{-2}) resulted in the most significant bacterial reduction (0.88 log CFU g^{-1}) after 6 days of storage, surpassing treatments with nHWEO alone and the combination with UV-C LED (0.63 and 0.68 log CFU g^{-1}, respectively). These results highlight the superior antibacterial effects of UV-C LED and the impact of nHWEO nanoemulsions when combined with non-thermal technologies. Although the combination of treatments resulted in a subadditive effect, this behavior may reflect complex interactions between the physicochemical mechanisms of action. Thus, the study highlights not only the individual potential of these approaches but also the relevance of exploring combined strategies to develop more sustainable and adaptable solutions for preserving plant-based foods.

Received 21st October 2025
Accepted 10th February 2026

DOI: 10.1039/d5fb00712g

rsc.li/susfoodtech

Sustainability spotlight

This study demonstrates a sustainable breakthrough by combining a linalool-rich Ho Wood essential oil nanoemulsion with non-thermal UV-C LEDs to inactivate *Staphylococcus aureus* in a plant-based burger. Mercury-free, low-energy LEDs promote efficient processing and maintain quality without intense heating. Nanostructuring improves the availability of the active ingredient and enables lower effective doses, contributing to formulations with fewer additives. The results support responsible production and consumption practices, strengthen health and well-being by increasing microbiological safety, and drive industrial innovation with clean and scalable technologies.

1 Introduction

Meat analogue products have emerged as a significant innovation in the food sector, offering protein alternatives that aim to replace or complement traditional animal-based sources. These analogues, predominantly formulated from plant-based proteins such as soy, rice, and peas, are designed to mimic the sensory, functional, and nutritional characteristics of conventional meat. Their growing acceptance is related to multiple factors, including environmental concerns associated with intensive livestock farming, such as greenhouse gas emissions, overuse of natural resources, and loss of

[a]*Center for Food Analysis (NAL), Technological Development Support Laboratory (LADETEC), Federal University of Rio de Janeiro, Chemistry Institute, Brazil. E-mail: dutra@iq.ufrj.br*

[b]*Laboratory of Advanced Analysis in Biochemistry and Molecular Biology (LAABBM), Federal University of Rio de Janeiro, Chemistry Institute, Brazil*

[c]*Graduate Program in Chemistry (PGQu), Institute of Chemistry (IQ), Federal University of Rio de Janeiro, Brazil*

[d]*Graduate Program in Food Science (PPGCAL), Institute of Chemistry (IQ), Federal University of Rio de Janeiro, Brazil*

[e]*Graduate Program in Biochemistry (PPGBq), Institute of Chemistry (IQ), Federal University of Rio de Janeiro (UFRJ), Brazil*

biodiversity, as well as ethical considerations regarding animal welfare.[1] In 2024, the global plant-based meat market was estimated at US $16.69 billion. According to the IMARC Group's projections, this market is expected to reach US $100.31 billion by 2033, representing a compound annual growth rate (CAGR) of 21.92% between 2025 and 2033. In the current scenario, North America leads the sector, with a 36.2% market share, reflecting the high demand for sustainable protein alternatives and the consolidation of consumers with profiles aligned with plant-based diets.[2]

In parallel with advances in innovation, the food industry has focused on developing novel preservation strategies in recent years, aiming to replace or complement traditional methods, such as synthetic preservatives and heat treatments.[3] Although these methods are effective and well-established in the production chain, several limitations have been associated with their continued use, including potential toxicological effects attributed to certain chemical additives and the occurrence of undesirable changes in the physical, chemical, and sensory composition of foods. These modifications can compromise the integrity of the food matrix, affecting characteristics such as flavor, texture, color, and nutritional stability.[4,5] In general, plant-based meat analogue products are formulated without the addition of traditional preservatives and rely primarily on maintaining the cold chain, particularly freezing at temperatures around −20 °C, as their primary preservation strategy. This limitation in adopting additional antimicrobial barriers can pose a challenge to microbiological safety during distribution and storage.[6] With the increased demand for alternative protein sources, coupled with the expansion of industrial-scale production, the risk of microbiological contamination during the formulation, handling, and packaging stages increases. Furthermore, the nutritional composition of these products, rich in proteins, lipids, and high-water activity, can create a favorable environment for the growth of spoilage and pathogenic microorganisms if additional control measures are not adopted.[7]

Nanoemulsions have emerged as a promising strategy for optimizing the application of essential oils and their isolated compounds, whose antimicrobial activity is widely recognized in the scientific literature. A significant limitation of essential oils in their free form is the need for high concentrations to achieve antimicrobial efficacy, which can compromise food sensory acceptability.[8] Furthermore, essential oils often exhibit low solubility in food systems with high water activity, where bacterial growth is favored. This limitation reduces their ability to reach and inhibit microbial growth in the food matrix uniformly. The use of surfactants such as Tween 80 facilitates nanoemulsification by stabilizing the interface between the oil and aqueous phases. The surfactant reduces the interfacial tension between the hydrophobic and aqueous phases, allowing the formation of nanometer-sized droplets upon application of mechanical shear. As a result, nanoemulsions provide a more uniform and stable dispersion of essential oils, facilitating their antimicrobial action in aqueous systems.[9]

Nanoemulsions are colloidal systems composed of two immiscible phases, stabilized by emulsifiers, whose dispersed droplets have average hydrodynamic diameters of less than 200 nm. This reduced diameter provides the system with high physical and chemical stability, a larger surface area for contact, and enhanced bioavailability of the active compounds.[10] Several *in vitro* and food matrix studies have reported considerable antimicrobial activity of essential oil nanoemulsions against foodborne pathogens.[11–13] Unlike microemulsions, which are thermodynamically stable, nanoemulsions are thermodynamically unstable but exhibit high kinetic stability. This is because the free energy of formation is positive, as the reduction in interfacial tension is not sufficient to compensate for the large interfacial area created. However, their long-term stability is governed by the droplets' minimal size, which promotes intense Brownian motion. The kinetics of Brownian motion reduce the influence of gravitational forces on the system, effectively delaying destabilizing mechanisms such as coalescence and Ostwald ripening for extended periods.[14,15]

Another emerging preservation method is irradiation with UV-C light from light-emitting diodes (LEDs), a technology that emits short-wavelength ultraviolet radiation (200–280 nm). The antimicrobial mechanism of action primarily involves the induction of irreversible damage to microbial DNA through the formation of pyrimidine dimers, which inhibit cell replication and lead to the death of the microorganism.[3] The application of UV-C LED has been widely investigated as a non-thermal alternative for preservation in several food matrices, due to its efficiency, low energy consumption, and lack of residue. However, its use in plant-based meat analogue products remains scarce, with few studies evaluating its microbiological efficacy.[6,16]

In this context, the present study aimed to evaluate the effectiveness of combining emerging preservation technologies, specifically the nanoemulsion of Ho Wood (*Cinnamomum camphora*) essential oil combined with UV-C LED irradiation, as an alternative for the microbiological preservation of plant-based burger analogues. The selected target pathogen was *Staphylococcus aureus*, a microorganism frequently associated with cross-contamination from improper handling and contaminated surfaces, and recognized for its role in foodborne illnesses.

2 Materials and methods

2.1. Materials

Ho Wood (*Cinnamomum camphora*) essential oil originates from China and was purchased from Ferquima Ltda (São Paulo, Brazil). The oil was obtained by steam distillation of the wood, with a density of 0.862 g cm^{-3} (20 °C), a refractive index of 1.4609 (20 °C), and the main constituent being linalool (98.83%), according to the manufacturer's technical report. Tween 80 (Isofar, Brazil), used as a surfactant, was purchased from Rei-Sol (Rio de Janeiro, Brazil). The additives, including guar gum, carboxymethyl cellulose, and meat-flavored seasoning, were purchased from Adicel (Minas Gerais, Brazil). Rice protein was purchased from Growth Supplements (Santa Catarina, Brazil). Texturized pea protein was obtained from Avante Food Systems (São Paulo, Brazil). The other seasonings added to the burger analogue formulation were purchased from local markets. *Staphylococcus aureus* ATCC 13565 was obtained from the culture stock of the Oswaldo Cruz Foundation (FIOCRUZ, Brazil).

2.2. Development of the nanoemulsion

The base formulation of the nanoemulsion was prepared by adding 1.0% Ho Wood essential oil, 3.0% Tween 80, and 96% ultrapure water (Mili-Q IQ 7005, Merck, Darmstadt, Germany), following the processing conditions described by da Silva *et al.*[14] Tween 80 was selected due to its approval for use in food and its safety, as certified by regulatory agencies such as the Food and Drug Administration (FDA). Tween 80 also has a high hydrophilic-lipophilic balance (HLB = 15.0), which favors the formation of more stable emulsions in aqueous systems.

To prepare 100 mL of the nanoemulsion, ultrapure water was initially added to a beaker, followed by Ho Wood essential oil. The water-essential oil system was then sheared in an Ultra-turrax rotor/stator (T25, IKA®, Staufen, Germany) operating at 7000 rpm. Tween 80 was gradually introduced into the rotating system, and the processing time was timed for 4 minutes after complete surfactant addition. The Ultraturrax was operated at 500 W using a model S25N-25G dispersion shaft (IKA®, Staufen, Germany). The equipment specifications include a 17 mm-diameter rotor, a 25 mm-diameter stator, and a 0.5 mm gap between the rotor and stator. The total length of the dispersion shaft is 194 mm, and the immersion depth of the shaft in the emulsion was adjusted to 35 mm.

2.3. Evaluation of diameter, polydispersity index, and zeta potential of nanoemulsions

The droplet diameter, polydispersity index (PDI), and zeta potential of the Ho Wood essential oil nanoemulsion (nHWEO) were determined by dynamic light scattering (DLS) using a Zetasizer LAB (Malvern Instruments, Malvern, UK) instrument. DLS is based on the analysis of Brownian motion, allowing the calculation of the mean particle diameter using the Stokes–Einstein equation.

To determine these parameters, the nanoemulsion samples were diluted 1 : 10 in ultrapure water (Mili-Q IQ 7005, Merck, Darmstadt, Germany) to ensure that the particle concentration was within the equipment's optimal detection range and to avoid excessive multiple scattering, which could interfere with the measurements. Measurements were performed at 25 °C. Droplet diameter and PDI measurements were performed using disposable polystyrene cuvettes (DTS 0012, Malvern Instruments, Malvern, UK), which are suitable for analyzing liquid dispersions at low concentrations. Zeta potential measurements were performed using disposable capillary cuvettes (DTS 1060, Malvern Instruments, Malvern, UK), which are designed to measure particle mobility in an electric field. The average values were obtained from three independent measurements.

2.4. Evaluation of nanoemulsion stability over time

The formulated nanoemulsions were evaluated for physicochemical stability over 38 days of storage at 25 °C (room temperature) and 4 °C (refrigeration). The analyses were performed on days 0, 7, 14, 21, and 38, with determination of the mean droplet diameter, polydispersity index (PDI), and zeta potential. On the day of preparation, the samples were also subjected to different physical treatments to simulate extreme processing and storage conditions. These treatments included heating to 75 °C for 5 minutes, freezing at −20 °C for 24 h, and then complete thawing. After each of these treatments, the samples were re-analyzed for droplet diameter, PDI, and zeta potential to assess potential changes in colloidal stability resulting from exposure to thermal and freezing stresses.

2.5. *In vitro* antibacterial activity

Staphylococcus aureus ATCC 13565 strains were activated in Brain Heart Infusion broth (Kasvi, Spain) by incubation at 37 °C for 24 hours. After incubation, the culture was centrifuged at 3218 × *g* for 5 minutes, and the supernatant was discarded. The pellet obtained was resuspended in sterile 0.85% (w/v) saline, and the cell suspension was read in a UV-1900i spectrophotometer (Shimadzu Corporation, Kyoto, Japan) at 625 nm until reaching an absorbance of 0.25, corresponding to an estimated concentration of 8.0 log CFU mL^{-1} (confirmed on a Plate Count Agar). This suspension was diluted in saline to a final concentration of 6.0 log CFU mL^{-1}, which was used in the assays to determine the minimum inhibitory concentration.

The minimum inhibitory concentration (MIC) assay against *Staphylococcus aureus* was conducted according to a methodology adapted from da Silva *et al.*,[17] using the broth microdilution method in sterile 96-well U-bottom microplates (Olen, China). To each well, 100 μL of previously sterilized Mueller–Hinton broth (Kasvi, Spain) was added. From a stock solution of nHWEO at 8.62 mg mL^{-1}, 100 μL was added to the first well of the microplate. The contents were carefully homogenized, and then 100 μL of the mixture was transferred to the next well, repeating the process until the last well. This process resulted in a serial dilution with a factor of two at each step, reducing the compound concentration by a factor of 2. The same procedure was adopted for the Ho Wood essential oil in non-nanoemulsified form. 100 μL of each bacterial suspension (6 log CFU mL^{-1}) was added to each well to reach a final concentration of approximately 5.5 log CFU mL^{-1}. Bacterial counts were confirmed on plate count agar (Kasvi, Spain) at the time of testing. The final concentrations evaluated in the wells after addition of the bacterial solution were 4.31, 2.15, 1.07, 0.54, 0.27, and 0.13 mg mL^{-1}.

The microplates were incubated at 37 °C for 24 hours under static conditions. At the end of the incubation period, the minimum inhibitory concentration (MIC) was determined as the lowest concentration of the tested compound that visibly inhibited bacterial growth, as evidenced by the absence of turbidity in the microplate wells. To validate the assay, appropriate controls were included: wells containing only Mueller–Hinton broth supplemented with 3.0% Tween 80, serving as a sterility control, and wells containing Mueller–Hinton broth with 3.0% Tween 80 and bacterial inoculum, serving as a positive growth control.

2.6. Formulation of plant-based burger analogues and physicochemical characteristics

The formulation of the burger analogues is described in Table 1. Initially, the previously weighed pea protein was hydrated in drinking water for 20 minutes at a 1 : 1 (w/w) ratio. After the

Table 1 Formulation of plant-based burger analogues[a]

Ingredients	Control burger analogue	nHWEO burger analogue
Water	30%	—
Textured pea protein	30%	30%
Rice protein isolate	12%	12%
Coconut fat	7.0%	7.0%
Bamboo fiber	4.0%	4.0%
Corn starch	4.0%	4.0%
Meat-flavored seasoning	5.0%	5.0%
Smoked paprika	3.0%	3.0%
Cocoa powder	2.0%	2.0%
Beet powder	2.0%	2.0%
Carboxymethylcellulose	0.5%	0.5%
Guar gum	0.5%	0.5%
nHWEO	—	30%

[a] nHWEO: Ho Wood essential oil nanoemulsion (8.62 mg mL^{-1}).

hydration period, excess water was carefully removed. The dough preparation involved aseptically mixing the dry ingredients with hydrated pea protein. First, the rice protein was homogenized to serve as a protein supplement, thereby improving the product's technological characteristics and nutritional profile. Then, the remaining dry ingredients were incorporated into the dough. Subsequently, the remaining ingredients, such as coconut fat, sunflower oil, and water, were added individually and sequentially, respecting this order, to ensure a uniform dough and adequate consistency of the food matrix. In treatments containing the nHWEO, water was entirely replaced with the same, maintaining the total volume constant across formulations.

After homogenizing the dough, the burger analogues were molded and standardized to 40 g per unit. The products were then packaged in sterile sample bags (Kasvi, Spain) and stored frozen at −20 °C until subsequent testing.

The proximate composition of the burger analogues was determined using near-infrared (NIR) spectroscopy with the FoodScan 2 equipment (FOSS, Hilleroed, Denmark), which was configured with a standardized calibration kit for plant-based meat analogues. This system allowed simultaneous quantification of moisture, protein, lipid, ash, and carbohydrates using multivariate calibration models previously validated for matrices with similar composition and structure. The water activity of the plant-based burger analogues was measured using a portable water activity meter (Pawkit®, Meter Group Latam Ltda., Brasil).

2.7. Microbiological evaluation of plant-based burger analogues

For the intentional contamination assay of the burger analogues, *Staphylococcus aureus* ATCC 13565 strains were activated in Brain Heart Infusion broth (Kasvi, Spain) by incubation at 37 °C for 24 hours. After incubation, the culture was centrifuged at 3218 × *g* for 5 minutes, with the supernatant subsequently discarded. The pellet obtained was resuspended in sterile 0.85% (w/v) saline, and the cell suspension was read on a UV-1900i spectrophotometer (Shimadzu Corporation, Kyoto, Japan) at 625 nm until an absorbance of 0.25 was reached, corresponding to an estimated concentration of 8.0 log CFU mL^{-1}. The intentional contamination assay was based on a study by Osaili *et al.*[18]

The bacterial suspension, initially standardized to 8.0 log CFU mL^{-1}, was diluted in a previously sterilized 0.85% (w/v) sterile saline solution to a final concentration of 7.0 log CFU mL^{-1}. The burger analogues were then transferred to a laminar flow hood, which had been previously sanitized and sterilized by exposure to UV-C light, ensuring aseptic conditions during the procedure. Next, 400 μL of the bacterial suspension was applied to the surface of each burger analogue, and evenly distributed using a sterile L-shaped spreader to ensure controlled and homogeneous contamination. After application, the samples were left in the laminar flow hood for 15 minutes to allow bacterial cells to attach to the product matrix before proceeding with the experimental treatments. A microbiological analysis of burger analogue samples without intentional contamination did not detect *Staphylococcus aureus* contamination, showing counts below the method's detection limit (<10 CFU g^{-1}). The microbiological evaluation treatments were:

(i) Control – burger without added nHWEO and without UV-C LED application.

(ii) (nHWEO) – burger analogue with the addition of nHWEO with a final concentration of 2.59 mg g^{-1} (achieved by incorporating 30% (w/w) of the stock nanoemulsion into the burger formulation).

(iii) (UV-C) – burger analogue subjected to UV-C LED.

(iv) (nHWEO + UV-C) – burger analogue subjected to UV-C LED treatment and added with nHWEO with a final concentration of 2.59 mg g^{-1} (achieved by incorporating 30% (w/w) of the stock nanoemulsion into the burger formulation).

After the bacterial fixation period, the samples designated for UV-C LED treatments were individually placed in a 275 nm LED irradiator at a distance of 15 cm between the samples and the lamps (Black Box Smart®, Biolambda, Brazil). The irradiation intensity was adjusted to 1.77 mW cm^{-2}. Each burger analogue was irradiated for 180 seconds, resulting in an accumulated dose of 0.32 J cm^{-2}, as controlled by the equipment module. The conditions were based on a previous study by Mutz *et al.*[16]

Staphylococcus aureus counts were performed at time points 0 (before and after UV-C LED treatment), 24 hours, 48 hours, and 6 days of storage. Baird Parker agar supplemented with egg yolk tellurite (Kasvi, Spain) was used. Samples were inoculated into Petri dishes at various dilutions per spread plate and then incubated at 37 °C for 24 hours. After incubation, the colonies formed were counted and expressed in CFU g^{-1}.

2.8. Statistical analysis

Statistical data analysis was conducted using factorial ANOVA to evaluate the interaction between storage time and temperature on droplet diameter, polydispersity index (PDI), and zeta potential. ANOVA was applied to examine the main effects and interactions between these variables. Additionally, a factorial

ANOVA was performed to investigate the impact of storage time and antimicrobial treatments on the reduction of *S. aureus* load in plant-based burger analogues. For all tests, differences were considered significant at $p < 0.05$. The results are presented as means ± standard error. A paired-comparison *t*-test was applied when necessary to compare the results before and after treatment. The test was conducted at the 5% significance level ($p < 0.05$).

Linear regression analysis was used to establish the relationship between storage time and the increase in mean droplet diameter. The goodness-of-fit of the polynomial model was verified using the coefficient of determination (R^2 and adjusted R^2), and statistical significance was confirmed using the *F*-test. All analyses were performed using STATISTICA 10 software.[19]

3 Results and discussion

3.1. Physicochemical characteristics of the nanoemulsion

Table 2 shows the evolution of the mean droplet diameter of the nanoemulsions during storage at 4 °C and 25 °C. The analysis of droplet diameters showed that both temperature and storage time significantly influenced nanoemulsion stability, with an interaction between the factors ($F = 4.4902$; $p = 0.00272$). It was observed that, at the initial time (day 0), the system presented minimal diameters (17.16 ± 6.23 nm). Values below 20 nm are rarely reported in the literature and represent a significant advance in emulsification process efficiency, since such small droplets favor dispersion transparency, increased surface area, and greater interaction with the continuous medium.[15] During storage at 4 °C, the nanoemulsions exhibited significant droplet growth ($p < 0.05$), reaching a diameter of 46.84 ± 8.36 nm after 38 days. Despite the gradual increase, the system remained below 100 nm, with values significantly lower than those observed in conventional systems (<200 nm), indicating high kinetic stability.[20,21] With similar results, Mazarei and Rafati[22] developed carvacrol nanoemulsions using a high-speed shear homogenizer at 15 000 rpm for 5 minutes and achieved droplet diameters between 150 and 350 nm, with a surfactant-to-oil ratio of up to 3 : 1. In parallel, in a study by Shao *et al.*,[23] ultrasound was employed as a method to reduce the droplet diameter in eugenol essential oil nanoemulsions, achieving particle sizes ranging from 200 to 300 nm. Similarly, Liu *et al.*[24] used high-pressure homogenization to prepare cinnamon essential oil nanoemulsions, with particle diameters ranging from 100 to 150 nm. Considering the results obtained, it is important to highlight that high-shear-rate homogenization is a promising alternative for the development of nanoemulsions, offering lower implementation costs than other commonly used methods, such as ultrasound, high pressure, and microfluidization. Furthermore, it is a technique that has been little explored in the scientific literature.

From a kinetic perspective, decreasing the temperature reduces the average energy available in the system, thereby limiting droplet kinetics through Brownian motion and, consequently, reducing the frequency of collisions between droplets. At lower collision energy, droplets are less likely to overcome steric and electrostatic repulsion barriers, thereby preserving the system's integrity.[25] Furthermore, the dynamics of Ostwald ripening are strongly dependent on solute diffusion between the dispersed and continuous phases. At lower temperatures, both molecular mobility and oil solubility in the aqueous phase are reduced, which limits the transport of molecules from smaller to larger droplets and slows the progressive enlargement of the mean diameter. In contrast, at higher temperatures, increased kinetic energy intensifies diffusion, increases the frequency and intensity of interdroplet collisions, and accelerates the redistribution of oil molecules, explaining the observed faster growth in droplet diameter.[14,26] At

Table 2 Physicochemical parameters of nanoemulsions during storage at 4 °C and[a] 25 °C

Droplet diameter/current effect ($T \times S_t$): $F = 4.4902$, $p = 0.00272$		
Temperature	Storage days	Droplet diameter (nm)
4 °C	Day 0	17.16 ± 6.23[a]
4 °C	Day 7	14.89 ± 6.23[a]
4 °C	Day 14	15.94 ± 7.07[a]
4 °C	Day 21	28.62 ± 7.07[a]
4 °C	Day 38	46.84 ± 8.36[ab]
25 °C	Day 0	17.16 ± 6.23[a]
25 °C	Day 7	18.30 ± 6.23[a]
25 °C	Day 14	30.03 ± 6.61[ab]
25 °C	Day 21	52.75 ± 6.23[b]
25 °C	Day 38	98.74 ± 6.23[c]
Zeta potential/current effect ($T \times S_t$): $F = 5.5432$, $p = 0.00056$		
Temperature	Storage days	Zeta potential (mV)
4 °C	Day 0	−14.83 ± 1.15[a]
4 °C	Day 7	−8.05 ± 1.15[b]
4 °C	Day 14	−11.76 ± 1.22[a]
4 °C	Day 21	−6.72 ± 1.15[b]
4 °C	Day 38	−5.59 ± 1.15[b]
25 °C	Day 0	−14.83 ± 1.15[a]
25 °C	Day 7	−10.00 ± 1.15[ab]
25 °C	Day 14	−14.00 ± 1.22[a]
25 °C	Day 21	−5.68 ± 1.15[b]
25 °C	Day 38	−14.39 ± 1.15[a]
PDI/current effect ($T \times S_t$): $F = 1.8761$, $p = 0.12298$/current effect (T): $F = 7.4757$, $p = 0.00774$		
Temperature	4 °C	0.259 ± 0.02[a]
	25 °C	0.352 ± 0.02[b]
PDI/current effect ($T \times S_t$): $F = 1.8761$, $p = 0.12298$/current effect (S_t): $F = 19.474$, $p = < 0.001$		
Storage days	Day 0	0.136 ± 0.03[a]
	Day 7	0.205 ± 0.03[a]
	Day 14	0.231 ± 0.04[b]
	Day 21	0.539 ± 0.03[c]
	Day 38	0.417 ± 0.03[bc]

[a] T = Temperature; S_t = storage; values expressed as mean ± standard error. Means followed by the same letter in the column do not differ statistically from each other by Tukey's test ($p < 0.05$). For PDI, as no significant interaction between temperature and day was observed ($p \geq 0.05$), the factors were analyzed separately.

25 °C, more pronounced instability was observed, with the droplet diameter increasing significantly from 17.16 ± 6.23 nm to 98.74 ± 6.23 nm in 38 days ($p < 0.05$).

Zeta potential analysis revealed that both temperature and storage time significantly influenced the electrical charge of the nanodroplets, with an interaction between the factors ($F = 5.5432$; $p = 0.00056$). The zeta potential values of the nanoemulsions varied between approximately −15 mV and −5 mV during storage, both at 4 °C and 25 °C. Although there were minor fluctuations between times and conditions, no significant changes were observed that compromised the system's stability. In the scientific literature, zeta potential values greater than +30 mV or less than −30 mV are considered indicative of colloidally stable systems due to the predominance of electrostatic repulsion between the particles. However, when the values are within the range of −30 mV to +30 mV, electrostatic repulsion is insufficient to stabilize the system, with stability mainly attributed to steric mechanisms.[27] It is important to highlight that the zeta potential values observed in this study may be directly related to the agglomeration, flocculation, or creaming potential, phenomena that indicate the instability of colloidal systems. Values close to zero (within the range of −30 mV to +30 mV) indicate weaker repulsive forces, favoring interaction between particles. In this range, van der Waals forces can overcome electrostatic repulsion, inducing the agglomeration of smaller droplets, even if the steric effect of the nanoparticles prevents coalescence.[15,28] These phenomena may explain the increase in particle diameter during storage.

The moderate variations in zeta potential observed in the present study can be attributed to interfacial reorganization of the surfactant and to possible adsorption of ions from the aqueous medium over time. Tween 80, a nonionic surfactant, does not provide strong long-range electrostatic repulsion but stabilizes primarily through steric repulsion and hydration forces. Thus, even though zeta potential values remained close to −10 mV, the protection provided by the surfactant layer was sufficient to prevent rapid coalescence, as evidenced by the behavior of droplet diameters over time. Therefore, the small fluctuations observed in zeta potential values should not be interpreted as a loss of stability, but rather as a reflection of dynamic adjustments at the essential oil/water interface during storage.[28,29]

For PDI, no significant interaction between temperature and storage time was observed ($p \geq 0.05$), indicating that these factors acted independently on droplet diameter variability. Therefore, the effects were analyzed separately. The PDI is a dimensionless parameter derived from the correlation function fit in DLS analysis, ranging from 0 to 1. Values close to 0 represent a perfectly monodisperse system with a narrow, unimodal size distribution, while values close to 1 indicate high polydispersity and heterogeneity. In this study, the nanoparticle size distribution was unimodal, with a single narrow peak, confirming the efficiency of the high-energy homogenization process in producing a uniform colloidal system even at increasing droplet sizes (SI). Regarding temperature, mean PDI values were significantly lower at 4 °C (0.259 ± 0.02) than at 25 °C (0.352 ± 0.02). This suggests that refrigerated storage contributed to maintaining a more homogeneous droplet distribution, probably due to lower molecular mobility and the consequent reduction in the rate of collisions and coalescence, factors that tend to generate populations of different sizes. Regarding the time factor, a progressive increase in PDI was observed throughout storage, with values close to 0.14 initially and above 0.50 after 21 days. This behavior indicates that the initially homogeneous system underwent size redistribution, with the simultaneous formation of larger droplets (resulting from coalescence and Ostwald ripening) and smaller ones (remaining from the initial emulsification). This increase in heterogeneity is consistent with reports in the literature, which associate droplet growth with a reduction in complete surfactant interfacial coverage, favoring the partial fusion of some units.[30] In practice, increasing PDI represents a loss of system uniformity, which can negatively impact its kinetic stability and functional properties. Nanoemulsions with a PDI <0.25 are generally considered monodisperse and stable, while values around 0.5 indicate moderate heterogeneity.[31] Thus, while the reduced diameter and steric protection ensured good stability in the first few days, the increase in PDI points to the occurrence of destabilization in more extended storage periods, especially at 25 °C, although the average diameter remained below 100 nm, indicating that the system retained typical nanoemulsion characteristics even at the end of the evaluated period.

Fig. 1 shows the linear regression of droplet diameter growth during storage at 4 °C and 25 °C. Under both conditions, a significant positive correlation was observed between storage time and diameter increase, indicating that the system, although initially stable, underwent a progressive increase in droplet diameter over time.

The regression at 4 °C showed a slope of 0.773 nm per day ($R^2 = 0.87$), indicating reduced average daily growth and consistent with greater kinetic stability. This slower rate can be attributed to the lower available thermal energy, which reduces molecular mobility and the frequency of droplet collisions, thereby delaying phenomena such as coalescence and Ostwald ripening. However, the regression at 25 °C revealed a slope approximately three times greater (2.426 nm per day; $R^2 = 0.90$), confirming that high temperatures accelerate the physicochemical instability of the nanoemulsion. In this scenario, the increased kinetic energy of the particles intensifies interdroplet collisions, favoring the diffusion of oil molecules from the dispersed phase and resulting in a more pronounced increase in the average diameter.

The high coefficient of determination ($R^2 > 0.85$ under both conditions) indicates that the linear model adequately describes droplet growth kinetics over the evaluated period. These results corroborate previous findings that report the strong dependence of nanoemulsion stability on storage temperature, with greater preservation of physicochemical characteristics under refrigeration.[25,32] Thus, the regression analysis confirms that refrigeration is a crucial condition for prolonging the kinetic stability of the nanoemulsion, reducing the droplet growth rate by more than 60% compared to storage at room temperature.

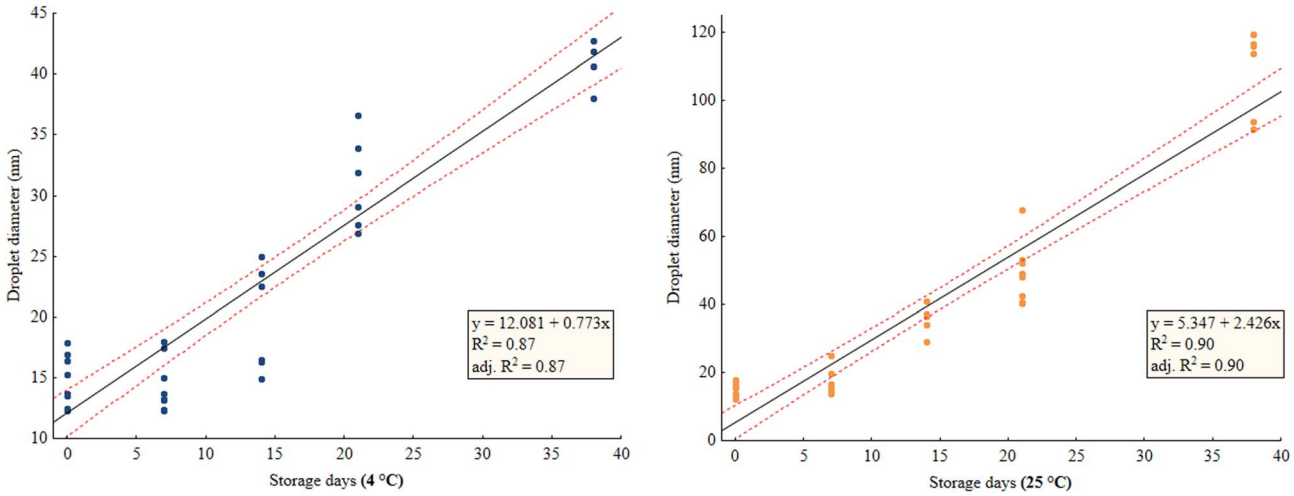

Fig. 1 Kinetics of increase in droplet diameter of nanoemulsions during storage.

Analysis of the physicochemical properties of Ho Wood essential oil nanoemulsions before and after heating and thawing reveals that these treatments significantly affect their stability (Table 3).

The observation of a considerable increase in droplet diameter after heating (from 16.96 nm to 55.33 nm) and thawing (from 16.96 nm to 82.81 nm) suggests that heat and temperature changes can accelerate droplet coalescence, a phenomenon in which smaller droplets merge to form larger droplets, thereby compromising the system's homogeneity. Furthermore, the increase in PDI after heating and thawing indicates greater heterogeneity in the system, which may lead to reduced stability over time. This may occur because, during these thermal processes, intermolecular forces may not be sufficient to maintain uniform droplet dispersion, resulting in wider dispersion. However, the zeta potential value only showed a significant difference during thawing ($p < 0.05$), suggesting that although the steric mechanism of the surfactant still stabilizes the system, thawing may affect the stability of the nanoemulsions more markedly.

3.2. *In vitro* antimicrobial activity

Table 4 presents the minimum inhibitory concentration values of Ho Wood essential oil in its free form and in nanoemulsified form against *Staphylococcus aureus*. The nanoemulsion inhibited bacterial growth at 4.31 mg mL^{-1}, whereas the free oil showed no inhibitory effect at the evaluated concentrations, indicating that nanostructuring enhanced antimicrobial activity. This result reinforces evidence from the literature suggesting that nanoemulsification of essential oils intensifies their antimicrobial activity, enabling use at lower concentrations and with a lower risk of compromising food sensory acceptance.[10]

The mechanism of action of essential oils against microorganisms is multifactorial and primarily involves the interaction of their hydrophobic constituents with cell membranes, leading to destabilization of the lipid bilayer, altered permeability, and consequent leakage of ions and essential macromolecules. Phenolic and terpenoid compounds present in essential oils can also interact with membrane proteins, cytoplasmic enzymes, and intracellular structures, leading to metabolic inhibition and cell death. However, in their free form, the effectiveness of this mechanism can be limited by their low aqueous solubility and tendency to volatilize or undergo

Table 4 Minimum inhibitory concentration of the Ho Wood essential oil nanoemulsion (nHWEO) and its non-nanoemulsified version against *S. aureus*

Treatments	*Staphylococcus aureus* ATCC 13565
nHWEO	4.31 mg mL^{-1}
Ho Wood essential oil	>4.31 mg mL^{-1}

Table 3 Physicochemical parameters of nanoemulsions during heating and thawing (day 0)[a]

	Heating (70 °C)			Thawing		
	Before	After	*p*-Value	Before	After	*p*-Value
Droplet diameter (nm)	16.96 ± 2.33	55.33 ± 18.40	0.003*	16.96 ± 2.33	82.81 ± 66.14	0.039*
PDI	0.146 ± 0.02	0.637 ± 0.29	0.044*	0.146 ± 0.02	0.296 ± 0.11	0.013*
Zeta potential (mV)	−14.83 ± 4.15	−14.22 ± 1.17	0.880	−14.83 ± 4.15	−7.06 ± 2.62	<0.001*

[a] Values followed by an asterisk (*) indicate significant differences ($p < 0.05$) between treatment conditions (before and after heating or thawing) for each parameter evaluated.

oxidative degradation. Nanoemulsification directly contributes to overcoming these limitations.

The scientific literature reports that nanoemulsions enhance the antimicrobial activity of essential oils, even at relatively low concentrations.[9,12,14] The increase in antimicrobial efficacy, despite the essential oil concentration being only 1%, can be attributed to the nanostructuring of the oil. By reducing the droplet size to the nanometer scale, the surface area of the active compound increases significantly, providing a larger interface for interaction with microbial cell membranes. This increased surface area allows for more efficient diffusion of the essential oil into the bacterial cell, thus increasing its antimicrobial potency. Furthermore, nanoemulsification improves the bioavailability of the essential oil in aqueous systems, making it more available for interaction with target microorganisms. As a result, even at low concentrations, the essential oil's antimicrobial activity is amplified compared to its free form.[33] Furthermore, the greater colloidal stability conferred by the presence of nonionic surfactants protects the active compounds against volatilization and degradation, prolonging their antimicrobial activity.[12,33,34]

Despite growing interest in essential oils as natural alternatives for controlling foodborne pathogens, the literature on the antimicrobial activity of Ho Wood essential oil remains scarce. Most studies focus on better-known essential oils, such as oregano, rosemary, and thyme. Linalool, the main bioactive compound in Ho Wood essential oil, has demonstrated antimicrobial activity in *in vitro* studies. In a study by Prakash and Vadivel *et al.*,[35] the antibacterial activity of nanoemulsion formulations against *Listeria monocytogenes* was evaluated, with the results showing that pure citral and linalool presented minimum inhibitory concentrations of 0.625% and 1.25%, respectively. However, the respective citral and linalool nanoemulsions showed twice the efficient antimicrobial activity, with MICs of 0.312% and 0.625%, respectively. These results indicate that nanoemulsification of these bioactive compounds enhanced their antibacterial efficacy, reducing the concentrations needed to inhibit bacterial growth. Alternatively, previous studies also showed a reduction in MIC after nanoemulsification of essential oils. Ramos *et al.*[13] found that *Origanum vulgare* essential oil had a MIC of 1.5 mg mL^{-1} against *Salmonella* Typhimurium, while its nanoemulsified form reduced this value to 0.59 mg mL^{-1}. Similarly, Sepahvand *et al.*[36] obtained twice the minimum inhibitory concentration values for the isolated compound thymol, indicating that the nanoemulsion was more effective in inhibiting the growth of *Escherichia coli*, *Staphylococcus aureus*, and *Clostridium perfringens*.

The differences in minimum inhibitory concentration values between the studies can be primarily attributed to the chemical composition of the essential oils used. Ho Wood essential oil has a virtually monocomponent composition, composed primarily of linalool (~98%). Linalool is an alcoholic monoterpene belonging to the oxygenated terpenoid class, characterized by its high lipophilicity and ability to interact with the lipid bilayer of bacterial membranes. This interaction can cause structural disorganization, increased permeability, and the leakage of ions and essential metabolites, leading to cell death. However, because it is an isolated compound, its action tends to be less potent compared to phenol-rich oils, such as carvacrol and thymol, which have greater antimicrobial activity due to their strong ability to denature proteins and destabilize membranes. Thus, the need for relatively higher concentrations of linalool to achieve an inhibitory effect, compared with other essential oils with different chemical compositions, explains the differences observed between the minimum inhibitory concentration of the Ho Wood essential oil nanoemulsion and those of other essential oils reported in the literature.[37,38]

3.3. Proximate composition of pea protein-based burger analogues

The proximate composition of the pea protein-based burger analogues showed no significant differences ($p \geq 0.05$) in moisture, protein, lipid, carbohydrate, or water activity contents between the conventional and nHWEO-added formulations (Table 5). These results indicate that incorporating the essential oil into the nanoemulsion did not substantially alter the main composition parameters, thereby preserving the product's nutritional profile. The only significant difference observed was in ash content, with slightly higher values in the nHWEO-added formulation. This increase may be related to the greater retention of mineral components during processing. However, no discussion of this is reported in the literature. Although the difference is slight, this result suggests that the addition of nHWEO can slightly influence the mineral fraction of the analogues, without compromising the other proximate composition characteristics.

Both formulations maintained a high protein content, comparable to or even higher than that reported for lean beef burgers.[39] The water activity (A_w) observed in the plant-based burger analogues was relatively low (0.88–0.89), lower than those generally reported for traditional burgers, which often have A_w values above 0.95 due to the higher free moisture content.[40] This reduction may be related to the interaction of water with protein and carbohydrate components present in plant-based formulations, restricting the availability of free water in the system. However, even with A_w below 0.90, microorganisms such as *Staphylococcus aureus* can still develop, as

Table 5 Proximate composition and water activity of raw plant-based burger analogues[a]

Composition	Analogue of a conventional burger (%)	Burger analogue added with nHWEO (%)
Moisture	48.73 ± 1.04	50.34 ± 1.39
Protein	24.94 ± 1.12	23.27 ± 1.44
Lipids	6.42 ± 0.02	6.62 ± 0.19
Ashes	3.79 ± 0.04[b]	3.89 ± 0.04[a]
Carbohydrates	16.07 ± 0.03	15.92 ± 0.19
Water activity	0.88 ± 0.03	0.89 ± 0.03

[a] nHWEO: Ho Wood essential oil nanoemulsion; means followed by different letters on the same line differ significantly from each other by the paired samples *t*-test ($p < 0.05$).

this bacterium can grow under conditions of low water availability, with growth limits reported around 0.86.[41] Thus, although analogues present a partial barrier to microbial proliferation compared to conventional meat products, microbiological safety is not fully assured, reinforcing the need for additional conservation and hygienic-sanitary control measures.

3.4. Microbiological evaluation

The factorial ANOVA revealed a significant interaction between treatment and storage time, demonstrating that the effect of treatments on microbial viability depends on the storage stage (Table 6). In the first hour (0–1 h), no differences were observed between groups, consistent with the absence of an immediate, detectable impact ($p \geq 0.05$). After 24 h, a consistent pattern was observed, with UV-C LED irradiation presenting the lowest *S. aureus* counts ($p < 0.05$). The control and the nHWEO-only version of the burger analogue presented the highest counts. By 48 h, all active treatments already differed from the control, although not among themselves. After six days of storage, the difference became more pronounced, with the UV-C LED treatment alone exhibiting the most significant reduction in bacterial viability, followed by nHWEO and nHWEO + UV-C LED at an intermediate level.

The superiority of UV-C LED in windows ≥24 h is supported in the literature by a combination of photoinduced damage to genetic material, such as the formation of pyrimidine dimers, and oxidative stress, both of which can reduce replicative capacity after exposure and throughout storage.[42] The antibacterial mechanism of UV-C LED action is primarily based on direct damage to the genetic material of bacterial cells. UV-C radiation (generally between 200 and 280 nm) is absorbed by the nitrogenous bases of DNA, forming pyrimidine dimers, such as thymine dimers. These dimers distort the DNA double helix, interfering with replication and transcription processes. Furthermore, UV-C radiation can generate reactive oxygen species, such as peroxides, which induce oxidation of cellular components, including lipids, proteins, and enzymes, leading to cell membrane rupture and compromising metabolic function. As a result, bacterial viability is drastically reduced, and the cell may be unable to reproduce or recover due to the genetic and structural damage induced by UV-C exposure.[43,44]

For treatment with the Ho Wood essential oil nanoemulsion (nHWEO), the initial latency and moderate reduction at later times are consistent with mechanisms reported for nanodroplets in food systems. Nanoemulsions with diameters below 40 nm can penetrate bacterial cells *via* passive diffusion, as their size allows them to interact with the lipid membrane. In Gram-negative bacteria, particles of this size range can cross the outer membrane *via* porins and reach the cell interior. In Gram-positive bacteria, as in the case of the pathogen studied, nanoemulsions can interact directly with the cytoplasmic membrane, potentially altering its integrity. When nanoemulsions reach the cell interior, they can release bioactive compounds, such as linalool in Ho Wood essential oil, and interfere with the cell's metabolic processes, including protein synthesis and energy production. The literature also indicates that efficacy can be modulated by physicochemical properties, such as diameter, shape, surface electrical charge, food matrix, and process parameters, which helps explain the detectable gain observed only after 48 h in our multiple comparisons.[45–48] Although the concentration of nHWEO incorporated into the burger (2.59 mg g^{-1}) was lower than the MIC determined in broth (4.31 mg mL^{-1}), an antimicrobial effect was still observed. This result can be explained by the fact that nanoemulsions, even at subinhibitory concentrations, can induce bacterial stress, compromise membrane integrity, and make cells more vulnerable to other preservation barriers. Furthermore, refrigeration can reduce the metabolic rate of *Staphylococcus aureus*, amplifying the impact of small physiological perturbations caused by the nanodroplets. The food matrix itself may also have played a significant role, acting as a reservoir and modulating the gradual release of linalool in microenvironments near the bacterial cells.[49,50]

An interesting effect observed in the present study was the difference in antibacterial activity between treatments with UV-C LED alone and those combined with a nanoemulsion. The combination of treatments reduced the antibacterial effect on plant-based burger analogues after 6 days of storage ($p < 0.05$). Although it is commonly hypothesized that combining two antimicrobials can potentiate their antibacterial effect, in the

Table 6 Effect of treatments on microbial viability during storage[a]

Microbial growth/current effect (treatment × S_t): $F = 6.1009$, $p = < 0.001$		
Treatment	Storage	CFU g^{-1}
Control	0 h	4.46 ± 0.094[a]
nHWEO	0 h	4.89 ± 0.094[a]
UV-C	0 h	4.57 ± 0.094[a]
nHWEO + UV-C	0 h	4.73 ± 0.094[a]
Control	1 h	4.52 ± 0.094[a]
nHWEO	1 h	4.85 ± 0.094[a]
UV-C	1 h	4.57 ± 0.094[a]
nHWEO + UV-C	1 h	4.55 ± 0.094[a]
Control	24 h	4.86 ± 0.094[a]
nHWEO	24 h	4.80 ± 0.094[a]
UV-C	24 h	4.18 ± 0.094[c]
nHWEO + UV-C	24 h	4.40 ± 0.094[b]
Control	48 h	5.19 ± 0.094[a]
nHWEO	48 h	4.79 ± 0.094[b]
UV-C	48 h	4.65 ± 0.094[b]
nHWEO + UV-C	48 h	4.58 ± 0.094[b]
Control	6 days	5.09 ± 0.094[a]
nHWEO	6 days	4.45 ± 0.094[b]
UV-C	6 days	4.21 ± 0.094[c]
nHWEO + UV-C	6 days	4.41 ± 0.094[b]

[a] S_t = storage days; control: sample of burger analogue without addition of nanoemulsion and UV-C LED; nHWEO: sample of burger analogue with addition of the Ho Wood essential oil nanoemulsion (concentration in the burger: 2.59 mg g^{-1}); UV-C: sample of burger analogue with application of UV-C LED at dose 0.32 J cm^2; nHWEO + UV-C: sample of burger analogue with addition of the Ho Wood essential oil nanoemulsion (concentration in the burger: 2.59 mg g^{-1}) and subjected to UV-C LED at dose 0.32 J cm^{-2}. Means followed by the same letter in the column do not differ statistically from each other by Tukey's test ($p < 0.05$).

present study, the nanoemulsion containing Ho Wood essential oil may have attenuated the efficacy of the UV-C LED due to an overlapping mechanism of action. The scientific literature on the combined use of these technologies is minimal, especially in the context of plant-based food products. Recent studies indicate that combining UV-C with nanoemulsions can be an effective strategy to reduce microbial load. For example, in a study by Mutz *et al.*,[16] optimizing the use of UV-C LED combined with an oregano essential oil nanoemulsion resulted in significant inactivation of *Salmonella* Enteritidis, with a reduction in the pathogen greater than that of the free essential oil, in addition to contributing to the minimization of lipid oxidation. Optimal conditions were achieved with a UV-C dose of 1752 mJ cm^{-2} and a nanoemulsion concentration of 8.50 mg mL^{-1}, resulting in a reduction of more than 1 log CFU with low oxidation (0.11 mg malondialdehyde per kg). Similarly, in a study by Yavari and Abbasi,[51] the combination of an oregano essential oil nanoemulsion (78.91 ppm) and aloe vera gel with UV-C irradiation (0.5 mJ cm^{-2}) demonstrated effective control of the microbial population in lentil sprouts during refrigerated storage, suggesting that the combined use of these technologies may offer significant benefits in the preservation of fresh foods. In the present study, the interaction between the two antimicrobial agents may have resulted in an antagonistic or subadditive effect, limiting the expected antibacterial impact. Linalool, the primary compound present in Ho Wood essential oil (>98%), is widely recognized for its antioxidant activity, as demonstrated in several antiradical assays, including DPPH$^{\bullet}$, ABTS$^{\bullet+}$, FRAP, and lipid peroxidation. This activity is attributed to its chemical structure, which consists of a monoterpene with a hydroxyl group linked to a cyclic ring, allowing the capture of free radicals and the inhibition of lipid peroxidation.[52–54] This mechanism of linalool can sequester reactive oxygen species generated in the extracellular environment, reducing the oxidative portion of the antibacterial effect of UV-C LED. However, the DNA photoproduct step remains a relevant consideration.

The temporal evolution confirms the treatment × storage days interaction observed in the factorial ANOVA and explains the effect size over time (Fig. 2). At 24 h, the UV-C LED alone showed the lowest count (≈4.19 log CFU g^{-1}), corresponding to a reduction of approximately 0.67 log units compared to the control (≈4.86 log CFU g^{-1}). At 6 days, the effect is accentuated, with the UV-C LED showing a reduction of approximately 0.88 log, followed by the combination of the nanoemulsion and UV-C LED (≈0.68 log) and the nanoemulsion alone (≈0.63 log), all

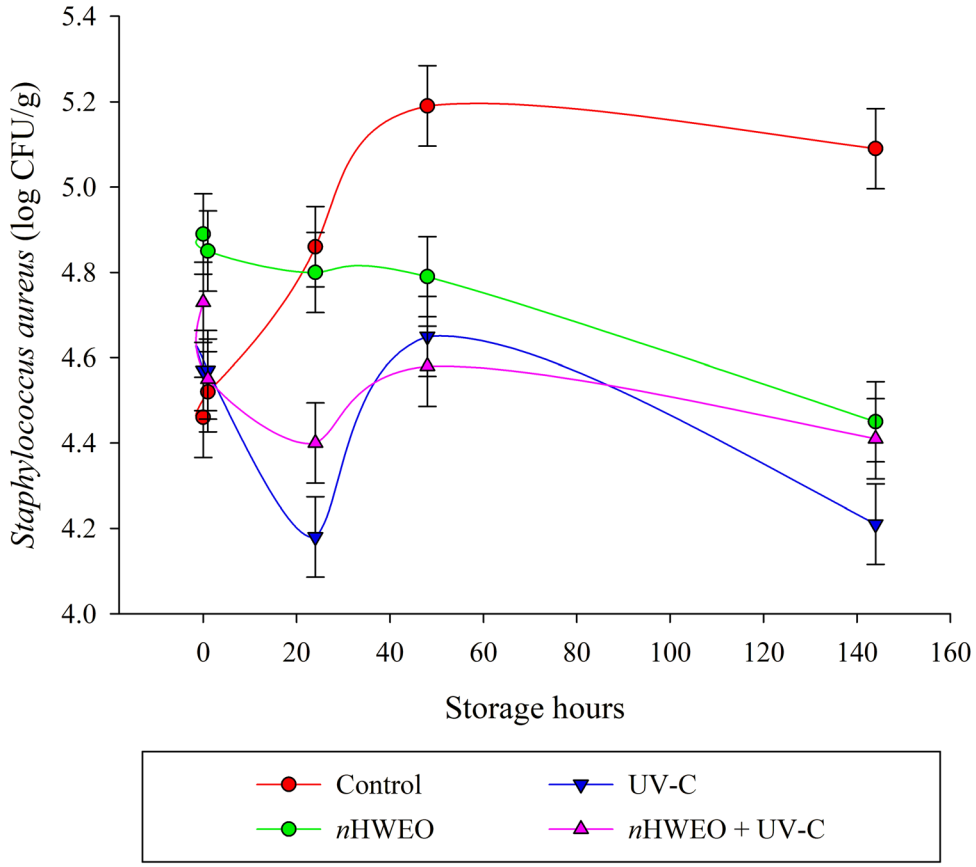

Fig. 2 Evolution of *S. aureus* count (log CFU mL^{-1}) over time in different treatments. Control: sample of burger analogue without addition of the nanoemulsion and UV-C LED; nHWEO: sample of burger analogue with addition of the Ho Wood essential oil nanoemulsion (concentration in the burger: 2.59 mg g^{-1}); UV-C: sample of burger analogue with application of UV-C LED at dose 0.32 J cm^{2}; nHWEO + UV-C: sample of burger analogue with addition of the Ho Wood essential oil nanoemulsion (concentration in the burger: 2.59 mg g^{-1}) and subjected to UV-C LED at dose 0.32 J cm^{-2}.

of which are below the control. A critical methodological aspect is the intentionally high inoculum, which tends to underestimate the relative impact of the treatments. The logarithmic reduction observed at a fixed dose may appear smaller than in real contamination scenarios, typically lower on food and industrial surfaces than the concentration tested in the present study. Under reduced and more realistic loads of *Staphylococcus aureus* contamination in food, the same treatment conditions as in the present study may produce a greater relative decrease and an earlier approach to the detection limit.

4 Conclusions

The study demonstrated the effectiveness of emerging preservation technologies, such as a Ho Wood essential oil nanoemulsion combined with UV-C LED radiation, in the microbiological preservation of plant-based burger analogues. The Ho Wood essential oil nanoemulsion significantly reduced the viability of *Staphylococcus aureus*, being more effective than the free form of the essential oil due to its greater relative surface area and colloidal stability, characteristics that enhance antimicrobial action.

The use of UV-C LED alone was more effective in inactivating microorganisms than its combination with the nanoemulsion, which can be attributed to the complex interplay of the mechanisms of action of both agents. The findings also demonstrate that, although UV-C LED has a substantial long-term antibacterial effect, with superior results after 24 hours, the Ho Wood essential oil nanoemulsion offers an additional benefit by allowing lower concentrations than the free essential oil. This demonstrates the potential of nanoemulsification as a crucial tool in improving the bioactivity of natural antimicrobial compounds.

In terms of innovation, the combined use of UV-C LED with nanoemulsions represents a promising approach for preserving plant-based food products, a growing area in the food sector. However, the interaction between the two methods requires further analysis, especially regarding the underlying biological mechanisms that may mitigate the expected efficacy. Although the combination of nHWEO and UV-C LED did not produce the expected synergistic antimicrobial effect, this interaction opens a promising avenue for food preservation. The ability of linalool-rich nanoemulsions to scavenge reactive oxygen species suggests that they may act as a protective barrier against the typical side effects of high-dose UV-C radiation. Future studies should investigate whether this combination can mitigate lipid and protein oxidation in food matrices, potentially enabling higher UV-C doses to ensure microbiological safety while maintaining the product's sensory and nutritional quality by attenuating oxidative damage.

Author contributions

da Silva, B. D.: conceptualization, investigation, formal analysis, writing – original draft, writing – review and editing; Mirres, A. C. M.: investigation, writing – original draft, writing – review and editing; Amaral, A. J. B.: investigation, writing – original draft, writing – review and editing; Ramos, C.: investigation, writing – original draft, writing – review and editing; Conte-Junior, C. A.: funding acquisition, project administration, writing – review and editing.

Conflicts of interest

There are no conflicts to declare.

Data availability

The manuscript contains all data necessary to support the findings, statements, and conclusions.

Supplementary information (SI) is available. See DOI: https://doi.org/10.1039/d5fb00712g.

Acknowledgements

The authors gratefully acknowledge the financial support provided by Fundação Carlos Chagas de Amparo à Pesquisa do Estado do Rio de Janeiro (FAPERJ) – grant number [E-26/200.059/2025]; Fundação Coordenação de Aperfeiçoamento de Pessoal de Nível Superior (CAPES), Brazil – grant number [88887.951413/2024-00; 88887.178900/2025-00]; and the Conselho Nacional de Desenvolvimento Científico e Tecnológico (CNPq) – grant number [140538/2025-9].

References

1 B. D. da Silva, J. M. da Costa Marques and C. A. Conte-Junior, *Food Human.*, 2025, **5**, 100734.
2 IMARC, *Plant-Based Meat Market Size, Share|Growth Report*, 2033, https://www.imarcgroup.com/plant-based-meat-market, accessed 1 July 2025.
3 D. K. A. Rosario, B. L. Rodrigues, P. C. Bernardes and C. A. Conte-Junior, *Crit. Rev. Food Sci. Nutr.*, 2020, **61**, 1163–1183.
4 A. M. Pisoschi, A. Pop, C. Georgescu, V. Turcuș, N. K. Olah and E. Mathe, *Eur. J. Med. Chem.*, 2018, **143**, 922–935.
5 N. A. N. A. El-Nabarawy, A. S. A. S. Gouda, M. A. M. A. Khattab and L. A. L. A. Rashed, *Environ. Sci. Pollut. Res.*, 2020, **27**, 14019–14032.
6 J. M. da Costa Marques, B. D. da Silva, A. J. B. do Amaral, G. H. M. Yi, L. Torres Neto, J. F. dos Santos Ferreira, M. L. G. Monteiro and C. A. Conte-Junior, *Food Human.*, 2025, **4**, 100621.
7 H. Valin, R. D. Sands, D. van der Mensbrugghe, G. C. Nelson, H. Ahammad, E. Blanc, B. Bodirsky, S. Fujimori, T. Hasegawa, P. Havlik, E. Heyhoe, P. Kyle, D. Mason-D'Croz, S. Paltsev, S. Rolinski, A. Tabeau, H. van Meijl, M. von Lampe and D. Willenbockel, *Agric. Econ.*, 2014, **45**, 51–67.
8 D. J. McClements, A. K. Das, P. Dhar, P. K. Nanda and N. Chatterjee, *Front. Sustain. Food Syst.*, 2021, **5**, 643208.
9 A. K. Pandey, M. L. Chávez-González, A. S. Silva and P. Singh, *Trends Food Sci. Technol.*, 2021, **111**, 426–441.

10 B. D. da Silva, D. K. A. do Rosario and C. A. Conte-Junior, *Crit. Rev. Food Sci. Nutr.*, 2022, **63**, 12567–12577.
11 K. Lei, X. Wang, X. Li and L. Wang, *Colloids Surf., B*, 2019, **175**, 688–696.
12 Y. Sun, M. Zhang, B. Bhandari and B. Bai, *Food Control*, 2021, **127**, 108151.
13 C. Ramos, Y. Mutz, B. D. da Silva, A. C. Ochioni, A. J. B. Amaral and C. A. Conte-Junior, *Int. J. Food Microbiol.*, 2025, **440**, 111273.
14 B. D. da Silva, C. A. Lelis, D. K. A. do Rosário, J. C. de Andrade and C. A. Conte-Junior, *Food Biosci.*, 2023, **55**, 103048.
15 S. M. Jafari and D. J. McClements, *Nanoemulsions: Formulation, Applications, and Characterization*, Academic Press, Massachusetts, 2018.
16 Y. S. Mutz, C. Ramos, M. L. Guerra Monteiro, B. Dutra da Silva, L. Torres, L. Tessaro and C. A. Conte-Junior, *Food Control*, 2023, **154**, 110004.
17 B. D. da Silva, C. A. Lelis, D. K. A. do Rosário, J. C. de Andrade and C. A. Conte-Junior, *Food Biosci.*, 2023, **55**, 103048.
18 T. M. Osaili, F. Hasan, D. K. Dhanasekaran, R. S. Obaid, A. A. Al-Nabulsi, M. Ayyash, L. Karam, I. N. Savvaidis and R. Holley, *Int. J. Food Microbiol.*, 2021, **337**, 108947.
19 StatSoft Inc., *Version 10*, 2011.
20 R. Moghimi, A. Aliahmadi, H. Rafati, H. R. Abtahi, S. Amini and M. M. Feizabadi, *J. Mol. Liq.*, 2018, **265**, 765–770.
21 Y. Ozogul, F. Ozogul, P. Kulawik, Y. Özogul, F. Özogul and P. Kulawik, *LWT*, 2021, **136**, 110362.
22 Z. Mazarei and H. Rafati, *LWT*, 2019, **100**, 328–334.
23 Y. Shao, C. H. Wu, T. T. Wu, Y. Li, S. G. Chen, C. H. Yuan and Y. Q. Hu, *Carbohydr. Polym.*, 2018, **193**, 144–152.
24 X. Liu, L. Chen, Y. Kang, D. He, B. Yang and K. Wu, *LWT*, 2021, **147**, 111660.
25 B. D. da Silva, D. K. A. do Rosário, D. A. Weitz and C. A. Conte-Junior, *Trends Food Sci. Technol.*, 2022, **121**, 1–13.
26 A. Jayari, F. Donsì, G. Ferrari and A. Maaroufi, *Foods*, 2022, **11**, 1858.
27 M. Koroleva, T. Nagovitsina and E. Yurtov, *Phys. Chem. Chem. Phys.*, 2018, **20**, 10369–10377.
28 L. Pavoni, D. R. Perinelli, A. Ciacciarelli, L. Quassinti, M. Bramucci, A. Miano, L. Casettari, M. Cespi, G. Bonacucina and G. F. Palmieri, *J. Drug Deliv. Sci. Technol.*, 2020, **58**, 101772.
29 A. S. Doost, D. Sinnaeve, L. De Neve, P. Van der Meeren, A. Sedaghat Doost, D. Sinnaeve, L. De Neve and P. Van der Meeren, *Colloids Surf., A*, 2017, **525**, 38–48.
30 C. D. Ferreira and I. L. Nunes, *Nanoscale Res. Lett.*, 2019, **14**, 1–13.
31 J. J. Pinelli, H. H. de A. Martins, A. S. Guimarães, S. R. Isidoro, M. C. Gonçalves, T. S. Junqueira de Moraes, E. M. Ramos and R. H. Piccoli, *LWT*, 2021, **143**, 111123.
32 H. D. Silva, M. A. Cerqueira and A. A. Vicente, *J. Food Eng.*, 2015, **167**, 89–98.
33 S. Gharenaghadeh, N. Karimi, S. Forghani, M. Nourazarian, S. Gharehnaghadeh, V. jabbari, M. S. khiabani and H. S. Kafil, *Food Biosci.*, 2017, **19**, 128–133.
34 S. Liao, G. Yang, Z. Wang, Y. Ou, S. Huang, B. Li, A. Li and J. Kan, *Ind. Crops Prod.*, 2022, **188**, 115654.
35 A. Prakash and V. Vadivel, *J. Food Sci. Technol.*, 2019, **57**(4), 1495–1504.
36 S. Sepahvand, S. Amiri, M. Radi and H. R. Akhavan, *Food Bioprocess Technol.*, 2021, **14**(10), 1936–1945.
37 B. D. da Silva, P. C. Bernardes, P. F. Pinheiro, E. Fantuzzi and C. D. Roberto, *Meat Sci.*, 2021, **176**, 108463.
38 K. Kachur and Z. Suntres, *Crit. Rev. Food Sci. Nutr.*, 2020, **60**, 3042–3053.
39 M. Serdarolu, H. S. Kavuan, G. Pek and B. Oztürk, *Korean J. Food Sci. Anim. Resour.*, 2018, **38**, 1.
40 B. D. da Silva, P. C. Bernardes, P. F. Pinheiro, J. Di Giorgio Giannotti and C. D. Roberto, *Food Biosci.*, 2022, **49**, 101896.
41 A. Austrich-Comas, C. Serra-Castelló, M. Viella, P. Gou, A. Jofré and S. Bover-Cid, *Foods*, 2023, **12**, 2199.
42 Y. S. Mutz, C. Ramos, M. L. Guerra Monteiro, B. Dutra da Silva, L. Torres, L. Tessaro and C. A. Conte-Junior, *Food Control*, 2023, **154**, 110004.
43 D. K. A. Rosario, B. L. Rodrigues, P. C. Bernardes and C. A. Conte-Junior, *Crit. Rev. Food Sci. Nutr.*, 2021, **61**, 1163–1183.
44 S. Bansaghi and J. Klein, *Infect. Prev. Pract.*, 2024, **6**, 100390.
45 L. S. Kato, C. A. Lelis, B. D. da Silva, D. Galvan and C. A. Conte-Junior, *Adv. Food Nutr. Res.*, 2023, **104**, 77–137.
46 M. Osanloo, A. Abdollahi, A. Valizadeh and N. Abedinpour, *Iran. J. Microbiol.*, 2020, **12**, 43–51.
47 A. S. Doost, D. Sinnaeve, L. De Neve, P. Van der Meeren, A. Sedaghat Doost, D. Sinnaeve, L. De Neve and P. Van der Meeren, *Colloids Surf., A*, 2017, **525**, 38–48.
48 K. Hou, Y. Xu, K. Cen, C. Gao, X. Feng and X. Tang, *Food Biosci.*, 2021, **43**, 101232.
49 C. Ramos, Y. Mutz, B. D. da Silva, A. C. Ochioni, A. J. B. Amaral and C. A. Conte-Junior, *Int. J. Food Microbiol.*, 2025, **440**, 111273.
50 S. Sepahvand, S. Amiri, M. Radi and H. R. Akhavan, *Food Bioprocess Technol.*, 2021, **14**(10), 1936–1945.
51 P. Yavari and H. Abbasi, *J. Food Meas. Char.*, 2021, **16**(1), 805–818.
52 A. Mutlu-Ingok, D. Devecioglu, D. N. Dikmetas, F. Karbancioglu-Guler and E. Capanoglu, *Molecules*, 2020, **25**, 4711.
53 J. P. Bautista-Silva, J. B. Seibert, T. R. Amparo, I. V. Rodrigues, L. F. M. Teixeira, G. H. B. Souza and O. D. H. H. dos Santos, *Curr. Microbiol.*, 2020, **77**, 2181–2191.
54 B. D. da Silva, P. C. Bernardes, P. F. Pinheiro, E. Fantuzzi and C. D. Roberto, *Meat Sci.*, 2021, **176**, 108463.

